GLP-1 Receptor Agonists and the Thyroid: C-Cell Effects in Mice Are Mediated via the GLP-1 Receptor and not Associated with RET Activation

Lars Wichmann Madsen,* Jeffrey A. Knauf,* Carsten Gotfredsen, Andrew Pilling, Ingrid Sjögren, Søren Andersen, Lene Andersen, Anne Sietske de Boer, Katia Manova, Afsar Barlas, Sushil Vundavalli, Niels C. Berg Nyborg, Lotte Bjerre Knudsen, Anne Marie Moelck, and James A. Fagin*

Novo Nordisk A/S (L.W.M., C.G., I.S., S.A., L.A., A.S.d.B., N.C.B.N., L.B.K., A.M.M.), Novo Allé, DK-2880, Bagsvaerd, Denmark; Memorial Sloan-Kettering Cancer Center (J.A.K., K.M., A.B., S.V., J.A.F.), New York, New York 10065; and Huntingdon Life Sciences (A.P.), Eye, Suffolk, IP23 7PX, United Kingdom

Liraglutide and exenatide are glucagon-like peptide receptor (GLP-1R) agonists used in the treatment of type 2 diabetes. Both molecules have been associated with the development of thyroid C-cell tumors after lifetime exposure in rodents. Previously, it has been reported that these tumors are preceded by increased plasma calcitonin and C-cell hyperplasia. We can now document that the murine C-cell effects are mediated via GLP-1R. Thus, 13 wk of continuous exposure to GLP-1R agonists was associated with marked increases in plasma calcitonin and in the incidence of C-cell hyperplasia in wild-type mice. In contrast, similar effects were not seen in GLP-1R knockout mice. Human C-cell cancer is often caused by activating mutations in the rearranged-during-transfection (*RET*) protooncogene. We developed an immunohistochemical method to assess *RET* activation in tissues. Liraglutide dosing to mice was not found to activate *RET*. Further evaluation of the signaling pathways demonstrated that liraglutide increased ribosomal S6, but not MAPK kinase, phosphorylation. These observations are consistent with effects of GLP-1R agonists on rodent C cells being mediated via mammalian target of rapamycin activation in a RET- and MAPK-independent manner. **(*Endocrinology* 153: 1538–1547, 2012)**

Glucagon-like peptide-1 receptor (GLP-1R) agonists are a new class of therapeutics for type 2 diabetes mellitus. Currently, two different agonists, liraglutide and exenatide, are on the market, and more are in clinical development (*e.g.* lixisenatide, albiglutide, and dulaglutide). In addition to glucose control, GLP-1R agonists offer potential additional therapeutic benefits including weight loss and reduced systolic blood pressure (reviewed in Ref. 1). The general pharmacology and clinical profile is similar among the different agonists (2, 3). Also, thyroid C-cell tumors have been described after 2-yr studies in rodents with both liraglutide (once daily) and exenatide (twice daily and once weekly) (4–6). With both GLP-1R agonists, plasma calcitonin increases and C-cell proliferative changes have been seen in mice after 13 wk of dosing, and lifelong treatment in rats was associated with C-cell cancer. In contrast, calcitonin increases or cellular proliferation was not seen in nonhuman primates (7), and no consistent difference between treatment groups were seen in the clinical program for liraglutide (8). This correlates with the observation that GLP-1R expression is low or absent in normal human thyroids (9). Thus, GLP-1R is consistently expressed in nonneoplastic and neoplastic C cells in rodents, whereas it is detected in only 27% of human C-cell neoplasms (9), suggesting species differences. Nevertheless, the findings have caused concern about the potential human thyroid safety of the GLP-1R agonist

ISSN Print 0013-7227 ISSN Online 1945-7170
Printed in U.S.A.

doi: 10.1210/en.2011-1864 Received October 10, 2011. Accepted December 14, 2011.
First Published Online January 10, 2012

* L.W.M., J.A.K., and J.A.F. contributed equally to the article.

Abbreviations: dpm, Disintegrations per minute; GDNF, glial cell line-derived neurotrophic factor; GLP-1R, glucagon-like peptide-1 receptor; GPCR, G protein-coupled receptor; IHC, immunohistochemistry; ISLB, *in situ* ligand binding; KO, knockout; LLOQ, lower limit of quantification; MTC, medullary thyroid cancer; mTOR, mammalian target of rapamycin; p, phosphorylated; pMEK, pMAPK kinase; RET, rearranged-during-transfection.

TABLE 1. Study design for animal experiments

Group	Strain of mouse	Treatment	Method of administration	Dose (mg/kg · d)	Animals (n)	
					Male	Female
1	GLP-1R KO	Liraglutide vehicle	Bolus sc	0	36	36
2	GLP-1R KO	Exenatide vehicle	Osmotic minipump	0	36	36
3	GLP-1R KO	Liraglutide	Bolus sc	3.0	36	36
4	GLP-1R KO	Exenatide	Osmotic minipump	3.0	36	36
5	CD-1 wild-type	Liraglutide vehicle	Bolus sc	0	36	36
6	CD-1 wild-type	Exenatide vehicle	Osmotic minipump	0	36	36
7	CD-1 wild-type	Liraglutide	Bolus sc	0.03	36	36
8	CD-1 wild-type	Liraglutide	Bolus sc	0.3	36	36
9	CD-1 wild-type	Liraglutide	Bolus sc	3.0	36	36
10	CD-1 wild-type	Exenatide	Osmotic minipump	3.0	36	36

class and led to implementation of precautionary measures around drug prescription (10). The present study further elucidates the rodent thyroid findings using mice as a model due to the previously described early onset of GLP-1R agonist-induced C-cell effects in this species (7).

In humans, C-cell cancer, or medullary thyroid cancer (MTC), is rare (11). Germline mutations in the rearranged-during-transfection (*RET*) protooncogene are associated with high penetrance of MTC in carriers, whereas approximately 50% of sporadic MTC have somatic mutations of RET (12). Upon RET activation, autophosphorylation takes place at key tyrosine sites in the protein. Phosphorylation, in particular at residue Y1062, is required for coupling to key downstream effectors of RET and for transformation (13, 14).

The actions of GLP-1 are mediated by a G protein-coupled receptor (GPCR) (15). In pancreatic β-cells, GLP-1 activates the mammalian target of rapamycin (mTOR) pathway by stimulating production of cAMP. Mobilization of intracellular Ca^{2+} stores by cAMP enhances mitochondrial activation to modulate K-ATP channels, which in the presence of other stimuli, such as glucose and amino acids, contributes to the activation of mTOR (16). Activation of mTOR in turn results in downstream phosphorylation of ribosomal S6 [phosphorylated (p)S6].

In the present study we assessed the GLP-1R dependency of the C-cell effects seen with liraglutide and exenatide through a study using GLP-1R knockout (KO) mice. We also investigated the association of hyperplasia and GLP-1R localization as well as the potential involvement of RET and of selected intracellular signaling pathways.

Materials and Methods

Animals

We used CD-1 mice (Crl:CD1; Charles River Ltd., Edinburgh, UK) aged 5–6 wk (n = 432) and GLP-1R KO mice (n = 288) lacking a functional GLP-1R, aged 4–5 wk [GLP-1R KO (CD-1 STOCK-FOXn1NU GLP1RTM1Ddr); Taconic Europe A/S, Lille Skensved, Denmark]. The animals were divided into 10 groups as outlined in the study design (Table 1). Animal experiments were conducted in accordance with national regulations and licenses granted by the United Kingdom Home Office. Animals were housed and handled according to current regulations, environmental enrichment was used throughout the study, and local animal ethics committee approval was obtained before study start.

Test articles

We purchased exenatide as freeze-dried powder (Exendin-4, catalog item H-8730; Bachem Distribution Services GmbH, Weil am Rhein, Germany). We produced liraglutide at Novo Nordisk A/S (Bagsvaerd, Denmark). We prepared solutions for injection in phosphate-buffered vehicles to achieve the desired concentration of active substance as verified by sampling and analysis using appropriate chromatographic methods (data not shown).

Dosing

All animals were dosed for 13 wk as described in Table 1. Dosing with liraglutide and liraglutide vehicle was done by daily sc injection rotating between dorsal injection sites. For dosing exenatide, which is very rapidly eliminated in mice, we implanted osmotic minipumps (Alzet 2006 model; ALZA Corp., Cupertino, CA) surgically on the back during general anesthesia. We replaced minipumps after approximately 7 wk to ensure continued drug exposure.

Bioanalysis

Before necropsy, after 13 wk, we drew blood from the ocular orbita and performed bioanalysis of EDTA plasma drug concentrations to confirm drug exposure (data not shown) by an ELISA [liraglutide, lower limit of quantification (LLOQ) = 40 pM] or liquid chromatography-mass spectrometry method (exenatide, LLOQ = 0.25 nM) and to determine plasma calcitonin concentrations. Calcitonin was measured by the use of a mouse calcitonin-specific immunosorbent radiometric assay (Immutopics International Inc., San Clemente, CA; catalog item 50-5000). Before spiking of calibrators and quality controls, neat mouse K2 EDTA plasma was incubated at 37 C for 96 h for removal of endogenous levels of calcitonin. Samples were assayed in accordance with manufacturer's instructions using

mouse calcitonin as reference (synthesis ID10062495; Abgent Inc., San Diego, CA). The LLOQ was 15 pg/ml. All assays were validated before use.

Necropsy

Animals were euthanized by carbon dioxide asphyxiation followed by exsanguination. Animals dosed with liraglutide were euthanized 2–3 h after the last dose. All animals were subject to a full macroscopical evaluation.

Tissue processing

Tissue processing for histopathology of the thyroid was initiated immediately after euthanasia. The entire thyroid gland was isolated on the trachea. The two lobes of the gland were separated by cutting longitudinally between the lobes. The right thyroid lobe was snap frozen and the left lobe fixed in 4% (vol/vol) paraformaldehyde. The pancreas was removed and frozen from animals in group 1 (GLP-1R KO) to serve as negative control for GLP-1R in the *in situ* ligand binding (ISLB) analysis.

The right thyroid and the pancreas were placed in O.C.T. compound (Tissue Tek; Sakura Finetek USA, Inc., Torrance, CA) in Cryomold molds (Sakura Finetek USA), small size ($7 \times 7 \times 5$ mm) (Tissue Tek), and frozen individually in isopentane cooled to approximately −80 C. Blocks with frozen right thyroid lobes from all mice were trimmed to expose thyroid tissue, and serial sections were made of nominally 10 μm thickness, starting at a point 600–700 μm caudal to the cranial pole of the gland. Where possible, a total of seven slides from each animal, each mounted with four frozen tissue sections, were used for the ISLB analysis.

The left thyroid lobe was fixed in paraformaldehyde for 20–36 h, processed, and paraffin embedded. Twelve tissue slides were prepared from each animal, with each slide containing four sections of a nominal thickness of 5 μm, starting at a point 600–700 μm caudal to the cranial pole of the gland. Two of these slides were stained by standard techniques with hematoxylin and eosin and immunohistochemistry (IHC) for calcitonin (7) and used for the histopathological diagnosis. The remaining slides were available for the pRET, pS6, and pMAPK kinase (pMEK) analyses.

Histopathological analysis

The sampling procedures secured that histopathological analysis was focused on the C-cell-rich region of the thyroid (7). Histopathological analysis was carried out by a board-certified veterinary pathologist, confirmed by blinded analysis, and peer reviewed. We followed diagnostic criteria from international guidelines within preclinical histopathology (17–19).

pRET, pS6, and pMEK IHC

IHC for phosphorylated proteins was performed on high-dose liraglutide animals and vehicle controls only. From each group, 11–12 mice with documented thyroid C-cell hyperplasia in the same thyroid lobe were examined for pRET, pS6, and pMEK. These parameters were assessed in both hyperplastic and normal C cells from thyroid tissue slices containing hyperplastic C cells.

As primary antibodies, we used anti-pRET Y1062 (catalog item sc-20252-R; Santa Cruz Biotechnology Inc., Santa Cruz, CA), anti-pS6 (S235/S236, catalog item 2211; Cell Signaling Technology Inc., Danvers, MA), and anti-pMEK (S217/S221, catalog item 9121; Cell Signaling Technology). As positive controls, we used TPC1 cells (gift from Dr. Sissy Jiang) (20) and MTC-M cells (American Type Culture Collection, Manassas, VA; CRL-1806) and Tg-RET/PTC transgenic mice, which express the oncoprotein selectively in thyroid cells (obtained from Dr. Jay Rothstein) (21). As negative controls, cells were treated with the RET kinase inhibitor AST487 (Novartis Pharma AG, Basel, Switzerland) using Western blots as standard (data not shown) (22). Additional negative controls included nonimmune IgG and incubation with secondary antibody alone. Briefly, TPC1 cells, which harbor an endogenous activated mutant of RET, were incubated for 24 h with vehicle or 500 nM AST487. MTC-M cells, which are derived from C cells and express wild-type RET, were incubated for 20 min with the RET ligand glial cell line-derived neurotrophic factor (GDNF; 0.2 μg/ml) and GDNF family receptor α-1 (GFRα1; 1.0 μg/ml), after a 30-min pretreatment with vehicle or 500 nM AST487. Cells were collected and aliquoted to prepare protein lysates for Western blotting or pelleted, fixed in paraformaldehyde, and embedded in paraffin for IHC analysis.

To quantify calcitonin- and pS6-positive cells, Metamorph software (Molecular Devices Inc., Sunnyvale, CA) was used. Total area covered by positive cells and negative cells was calculated. Total number of positive and negative cells was calculated dividing the total area of positive and negative staining for the respective antibody by the average area of the cells.

In situ ligand binding

We carried out ISLB on tissue sections as previously reported (7, 23). ISLB was performed on mid- and high-dose liraglutide animals and vehicle controls only. Before the ISLB assay, we demonstrated the presence of C cells by calcitonin staining (IHC) of adjacent sections. Thyroids containing C cells were incubated with radioactive [^{125}I]GLP-1 alone or with radioactive GLP-1 plus a 330-fold excess of nonradioactive GLP-1. After preincubation (15 min) and incubation (2 h), slides were washed with buffer, fixed with 2% glutaraldehyde, washed with water, incubated with 99% ethanol, and washed with water again. The slides were then costained for calcitonin by IHC.

For autoradiography, the slides were dipped in fluid LM-1 emulsion (GE Healthcare Europe GmbH, Brøndby, Denmark), dried overnight, stored with desiccant, and exposed for 7 d in the cold. The slides were brought to room temperature, developed in D19 (2 min), stopped with 1% acetic acid plus 1% glycerol (1 min), and fixed with 30% Na-thiosulfate (2 min) before the final water wash. The slides were counterstained in Mayer's hematoxylin, dehydrated, and mounted.

As positive controls for the calcitonin staining of the thyroid and for the ISLB, we used a set of slides with one cryostat section each of a rat thyroid and a mouse pancreas. Pancreas tissue sections were analyzed by a procedure identical to the ISLB/calcitonin staining procedure except that purified rabbit antihuman insulin antibody (AP08860PU-N; Acris Antibodies Inc., San Diego, CA) was used as primary antibody.

For each assay day, an ^{125}I standard [ARI 0133A (PL), low activity; American Radiolabeled Chemicals Inc., St. Louis, MO] was used for quantification. The standard was used to derive the disintegrations per minute (dpm) per square micrometer used as an indirect measure of GLP-1R density.

For quantification, slides were loaded into a slide scanner (Hamamatsu NanoZoomer 2.0HT; Hamamatsu Photonics KK,

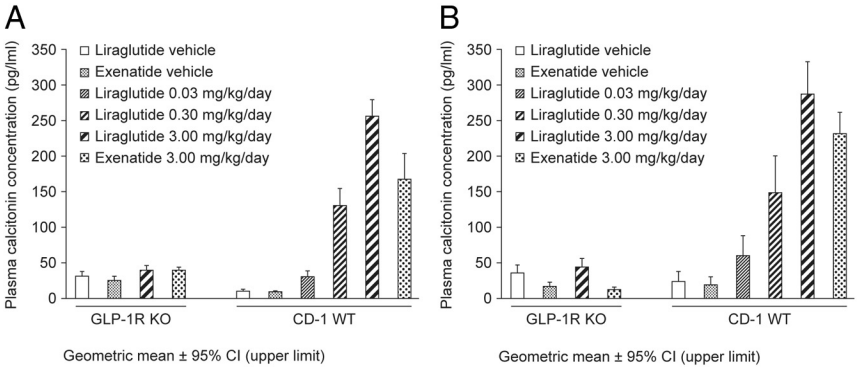

FIG. 1. Plasma calcitonin (picograms per milliliter) after 13 wk treatment, group geometric mean, and 95% confidence interval in male (A) and female (B) mice (n = 36 mice per sex per group). WT, Wild type.

Hamamatsu City, Japan), and three areas within the thyroid sections were framed for scanning using a ×40 objective. Images were subsequently imported into the image analysis program (Visiopharm Integrator System; Visiopharm A/S, Hørsholm, Denmark). Pictures of C-cell and non-C-cell areas were then acquired and analyzed. Areas with C cells, non-C cells, and background were identified and masked. Subsequently, silver grains in these masked areas were counted and the masked areas measured.

Statistical analyses

Data on calcitonin were log transformed before analysis and analyzed using a three-way ANOVA approach, with the three factors strain of mouse, treatment, and sex. Variance heterogeneity was included in the model. Each sex was analyzed separately, using contrasts and estimated differences. Calcitonin levels below the limit of quantification were treated as equal to 7.5 pg/ml, which was half the limit of quantification.

For data on thyroid C-cell histopathology, the proportion of animals with C-cell hyperplasia was analyzed using two-tailed Fisher's exact test for each treated group *vs.* the relevant control.

Data on pS6-positive C cells were compared between liraglutide (3 mg/kg · d) and vehicle-dosed controls using a Student's *t* test.

Data on GLP-1R density from the ISLB analysis were analyzed using a two-way ANOVA testing the effect of presence or absence of C-cell hyperplasia and an analysis testing the effect of liraglutide (vehicle or 0.3 or 3 mg/kg · d), sex, and interaction between liraglutide and sex.

For all statistical analyses, $P < 0.05$ was used as significance level.

Results

GLP-1R agonist-induced calcitonin increases are GLP-1R dependent

Plasma calcitonin levels in wild-type mice dosed with liraglutide at 0.03, 0.3, or 3.0 mg/kg · d were significantly higher than in vehicle controls ($P < 0.01$, $P < 0.001$, and $P < 0.001$ for the three doses, respectively) in both males and females (Fig. 1, A and B). In contrast, there was no statistically significant difference in plasma calcitonin between GLP-1R KO mice dosed with liraglutide at 3.0 mg/kg · d and vehicle controls. For exenatide, plasma calcitonin in wild-type mice dosed at 3.0 mg/kg · d was also significantly higher than in vehicle controls for both sexes ($P < 0.001$), whereas no consistent effect was observed in GLP-KO mice. Comparing the calcitonin response between strains statistically, the calcitonin increase in animals dosed with liraglutide or exenatide (3.0 mg/kg · d *vs.* vehicle) was significantly higher in wild-type mice compared with GLP-1R KO mice ($P < 0.001$ for both sexes and both compounds).

Liraglutide- and exenatide-induced C-cell hyperplasia in mice is GLP-1R dependent

When compared with vehicle controls, there was an increased incidence of C-cell hyperplasia in the thyroid gland of both sexes receiving 0.3 or 3.0 mg/kg · d liraglutide by bolus injection (Table 2). This increase was statistically significant in females receiving 3.0 mg/kg · d lira-

TABLE 2. Thyroid C-cell hyperplasia incidence in wild-type CD-1 and GLP-1R KO mice (n = 36 mice per sex per group) after 13 wk treatment with liraglutide or exenatide

	C-cell hyperplasia (n)					
			Liraglutide			
	Liraglutide vehicle, 0 mg/kg · d	Exenatide vehicle, 0 mg/kg · d	0.03 mg/kg · d	0.3 mg/kg · d	3 mg/kg · d	Exenatide, 3 mg/kg · d
CD-1 mice						
Males	1	0	1	10[a]	5	5
Females	0	0	0	8[a]	8[a]	9[a]
GLP-1R KO mice						
Males	0	0			0	0
Females	0	0			0	0

[a] $P < 0.05$ compared to relevant vehicle control.

glutide and in males and females receiving 0.3 mg/kg · d ($P < 0.05$). C-cell hyperplasia was also observed in mice receiving 3.0 mg/kg · d exenatide by continuous minipump administration ($P < 0.05$). The incidence of hyperplasia was similar in mice receiving exenatide or liraglutide (3.0 mg/kg · d). All cases of C-cell hyperplasia were diffuse in nature but localized to the cranial and central part of the gland. The hyperplasia generally consisted of an increase in the overall number of C cells but without the formation of significant focal C-cell aggregates (Fig. 2A and Supplemental Fig. 1, published on The Endocrine Society's Journals Online web site at http://endo.endojournals.org). The location of the calcitonin-staining cells is consistent with that observed by others. Indeed, rat C cells may be found in the stroma, between epithelial cells, or even in the lumen of follicles (24). Lindfors *et al.* (25) found a similar pattern in mouse thyroids. No other histopathological thyroid changes related to treatment were found.

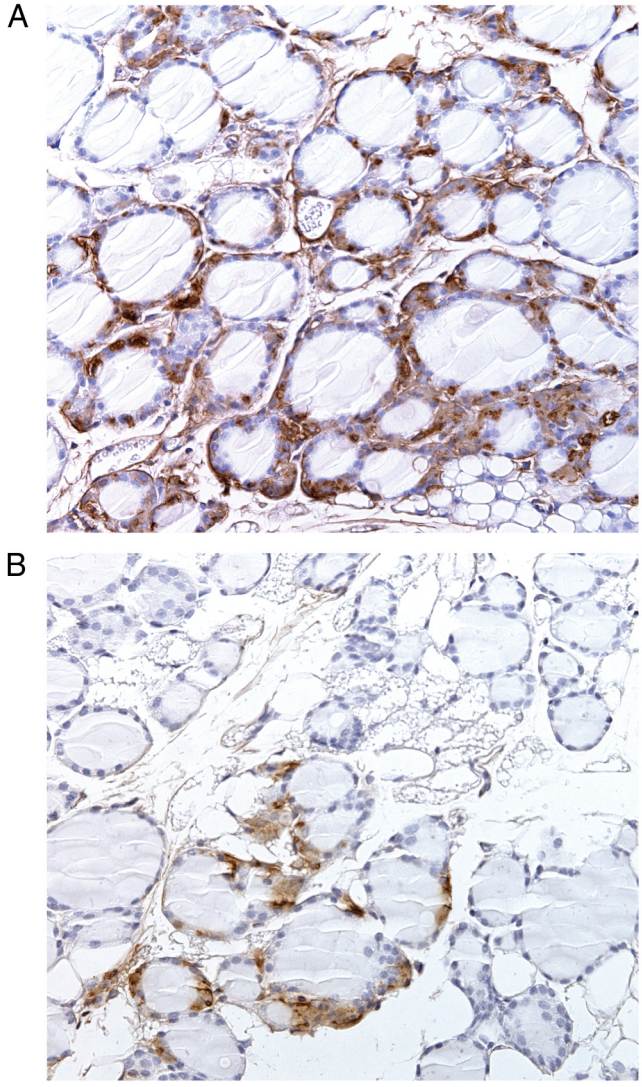

FIG. 2. Thyroid histology after 13 wk treatment with liraglutide (3 mg/kg · d) in CD-1 wild-type mice showing diffuse C-cell hyperplasia (A) and GLP-1R KO mice with normal C cells (B). Calcitonin IHC (*brown*), ×20 objective.

In contrast to the findings in wild-type mice, no changes were seen in the thyroid glands of GLP-1R KO mice. In particular, no evidence of C-cell hyperplasia was observed (Fig. 2B).

GLP-1R density in C cells in relation to liraglutide treatment

GLP-1 binding was found preferentially on C cells when ISLB was carried out on calcitonin-immunostained slides (Fig. 3, A and B). GLP-1R density was expressed as radioactivity per C-cell area (calcitonin stained) and was statistically significantly higher in mice dosed with liraglutide compared with vehicle controls (1.83 and 1.89 *vs.* 1.42 dpm/μm^2 C-cell area, for 0.3 and 3 mg/kg · d *vs.* vehicle; $P < 0.01$) (Fig. 3C). The specificity of the ILSB method for the presence of the GLP-1R was confirmed as specific binding was close to zero in slides from GLP-1R KO mouse thyroid (-0.02 ± 0.04 dpm/μm^2; n = 18) and pancreas (0.01 ± 0.03 dpm/μm^2; n = 29). In the frozen tissue sections available for the ISLB analysis, C-cell hyperplasia could be detected in slides from 10 mice. Within these sections, GLP-1R density in areas with C-cell hyperplasia was compared with areas without C-cell hyperplasia. There was no statistically significant difference in GLP-1R density between these areas.

Liraglutide-induced C-cell hyperplasia in mice is not associated with RET activation

IHC to detect pRET in tissue sections has not previously been described and was developed and validated as part of this study (Fig. 4). Titration of the RET pY1062 antibody on TPC1 cell pellets showed good resolution for IHC, with optimal concentration of 0.01–0.05 μg/ml (Fig. 4A), showing clear membrane staining, which was abolished in cells treated with the RET kinase inhibitor AST487. For additional validation, we performed IHC of MTC-M mouse medullary thyroid cancer cells, which express wild-type RET. Upon treatment with the RET ligand GDNF in the presence of the accessory protein GDNF family receptor α-1, there was an increase in RET phosphorylation as detected by IHC, which was inhibited by AST487 (Fig. 4B). As with the TPC1 cells, the optimal antibody concentration for detection of pRET (Y1062) was 0.01–0.05 μg/ml. Finally, we incubated thyroid sections from RET/PTC3 transgenic mice, which develop papillary thyroid cancers driven by the RET oncoprotein. IHC with pRET (Y1062) showed clear membrane staining at concentrations from 0.01–0.05 μg/ml, with 0.05 μg/ml also showing nonmembranous staining in normal thyroid follicular cells (Fig. 4C), which do not express RET. We next ex-

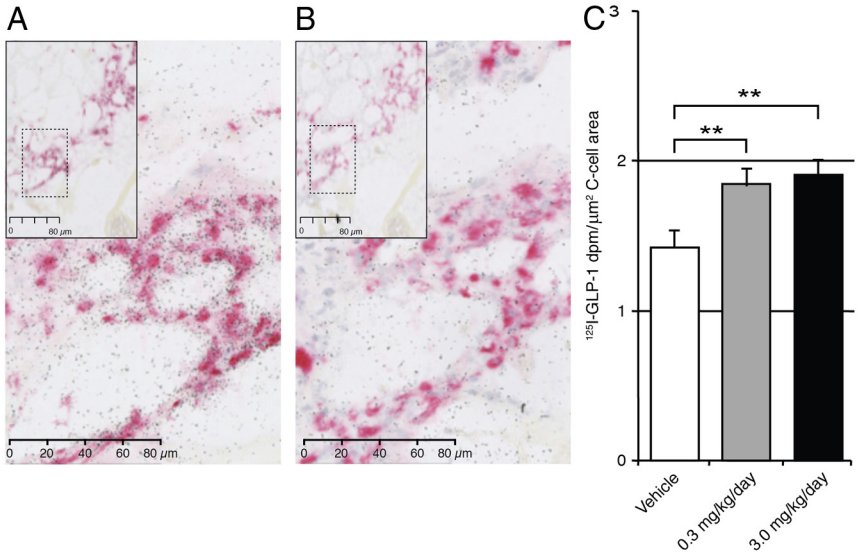

FIG. 3. GLP-1R ISLB on frozen sections of thyroid from mice. A and B, Mouse thyroid stained immunohistochemically for calcitonin (*pink*) and assessed by autoradiography for GLP-1R (black silver grains): A, incubated with 0.3 nM [^{125}I]GLP-1 (hot) to show the sum of bound ligand; B, incubated with 0.3 nM [^{125}I]GLP-1 plus 1 μM nonradioactive GLP-1 (cold) to compete out specific binding. The low-magnification *insets* illustrate that neighboring sections were used. C, After 13 wk treatment, GLP-1R density, that is, specific [^{125}I]GLP-1 binding (dpm) per calcitonin-positive area (square micrometers), was higher in mice dosed with liraglutide compared with vehicle controls. **, $P < 0.01$.

amined effects of the RET kinase inhibitor on MEK and S6 phosphorylation in TPC1 cells. AST487 inhibited phosphorylation of these effectors as determined by Western blotting (not shown), and the IHC stains in the cell pellets showed good resolution of these changes (Fig. 4D).

Based on these validation experiments, we then examined thyroid tissues from mice dosed with liraglutide (3 mg/kg · d) and compared the results to vehicle controls. IHC for pRET and for pMEK and pS6K was performed on tissue sections immediately contiguous to regions of C-cell hyperplasia or of normal C cells. We found no RET membrane staining in C cells in either liraglutide- or vehicle-treated mice with an antibody concentration of 0.01 μg/ml (Fig. 5A and Table 3). At a concentration of 0.05 μg/ml, the background staining was high. Even in these more sensitive, yet less specific, conditions, there was still no evidence of membrane staining in the C-cell-rich regions, as opposed to our findings in the controls.

There was an increase in pS6 staining in C cells of liraglutide-treated mice (Fig. 5B and Table 3). This effect was quantified by counting the number of pS6/calcitonin double-positive cells. As shown in Fig. 5C, there was an increase in the ratio of pS6/CT-positive cells in the liraglutide-treated mice compared with controls ($P < 0.05$). By contrast, there was no increase in pMEK staining in the liraglutide-treated animals (Fig. 5D and Table 3).

Discussion

The present study documents that GLP-1R agonists cause C-cell hyperplasia and calcitonin release in mice via a GLP-1R-dependent mechanism. The daily administration of liraglutide once daily or exenatide (pump infusion) for 13 wk at doses up to 3.0 mg/kg · d caused C-cell hyperplasia in wild-type mice but not in GLP-1R KO mice.

For the histopathological assessment of thyroid C-cell changes, the diagnostic criteria used in this study were based on guidelines designed for evaluation of 2-yr rodent carcinogenicity studies (17, 18). In view of the shorter duration of treatment in this study, C-cell adenomas and carcinomas were not expected to occur, and indeed such changes were not observed. Focal C-cell hyperplasia, defined as formation of aggregates of C cells, was also not observed; instead, the observed C-cell hyperplasia was diffuse in nature. Diffuse C-cell hyperplasia was characterized as an exaggeration of the normal pattern compatible with a response to continued physiological stimulation.

In wild-type mice, the administration of liraglutide and exenatide for 13 wk was previously shown to induce C-cell hyperplasia in approximately 40% of the animals when investigating both thyroid lobes (7). In the present study, the histopathological diagnosis of C-cell hyperplasia was based on investigating only one lobe, which reduced the likelihood of recording changes. This procedure was necessary to secure availability of the opposite lobe for ISLB analysis. Considering this unilateral examination, the observed incidence of C-cell hyperplasia of 14–25% in the high-dose liraglutide and exenatide groups was consistent with previous data (7). For both liraglutide and exenatide, this incidence in wild-type mice was statistically significantly higher compared with respective controls. In GLP-1R KO mice, no evidence of C-cell hyperplasia was observed.

GLP-1R dependency was also demonstrated for the observed increase in plasma calcitonin. For both liraglutide and exenatide, a calcitonin increase was seen only in wild-type mice but not in KO animals. The plasma calcitonin levels were higher in females than in males and higher in the KO animals than in the wild-type animals. Although the biological explanation for the sex differences is not known, these observations are

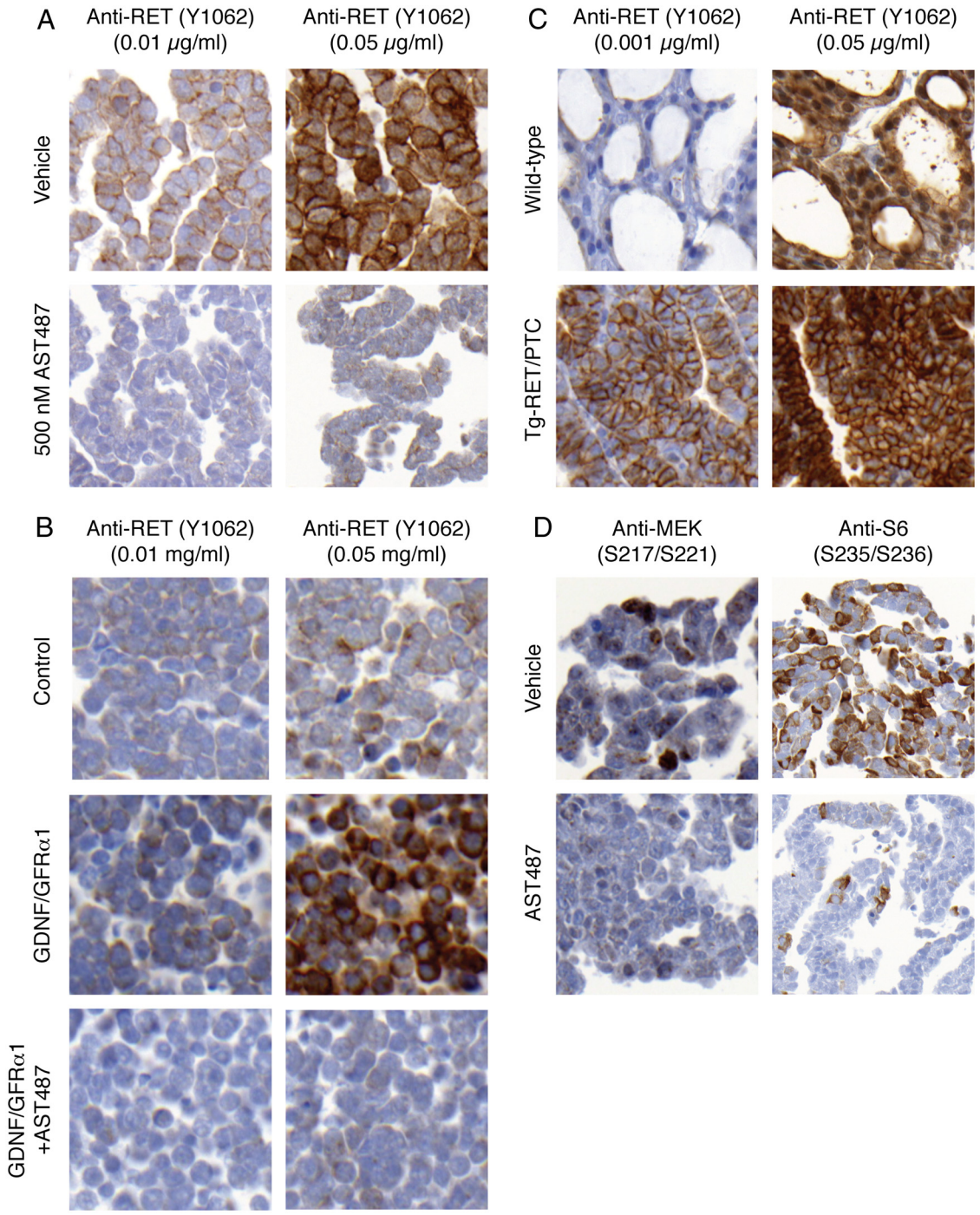

FIG. 4. Phosphoprotein IHC validation experiments. A, TPC1 cells were incubated for 24 h with vehicle or the RET kinase inhibitor AST487. IHC was done on sections of TPC1 cells using anti-RET (Y1062) at 0.01 or 0.05 μg/ml. B, pRET IHC in MTC-M cells expressing wild-type RET. IHC was done on paraffin sections of MTC-M cells using anti-RET (Y1062) at 0.01 or 0.05 μg/ml. C, pRET IHC in mouse papillary thyroid cancers expressing constitutively active RET. IHC was done on paraffin sections of MTC-M cells using anti-RET (Y1062) at 0.01 or 0.05 μg/ml. D, AST487 inhibits MEK and S6 phosphorylation as determined by IHC in TPC1 cells. IHC was done on paraffin sections of TPC1 cells with anti-MEK (S217/S221) at 0.2 μg/ml or anti-S6 (S235/S236) at 0.12 μg/ml.

consistent with results from previous studies (7). As also seen previously, increased calcitonin was observed at a dose of liraglutide (0.03 mg/kg · d) that did not induce C-cell hyperplasia. This observation confirms the sensitivity of plasma calcitonin to detect low-level C-cell stimulation induced by GLP-1R agonists in rodents. Thus, it confirms that C-cell activation and resulting calcitonin release precedes C-cell hyperplasia.

The objective of ISLB was to assess whether GLP-1 agonist treatment affected GLP-1R density in C cells. The

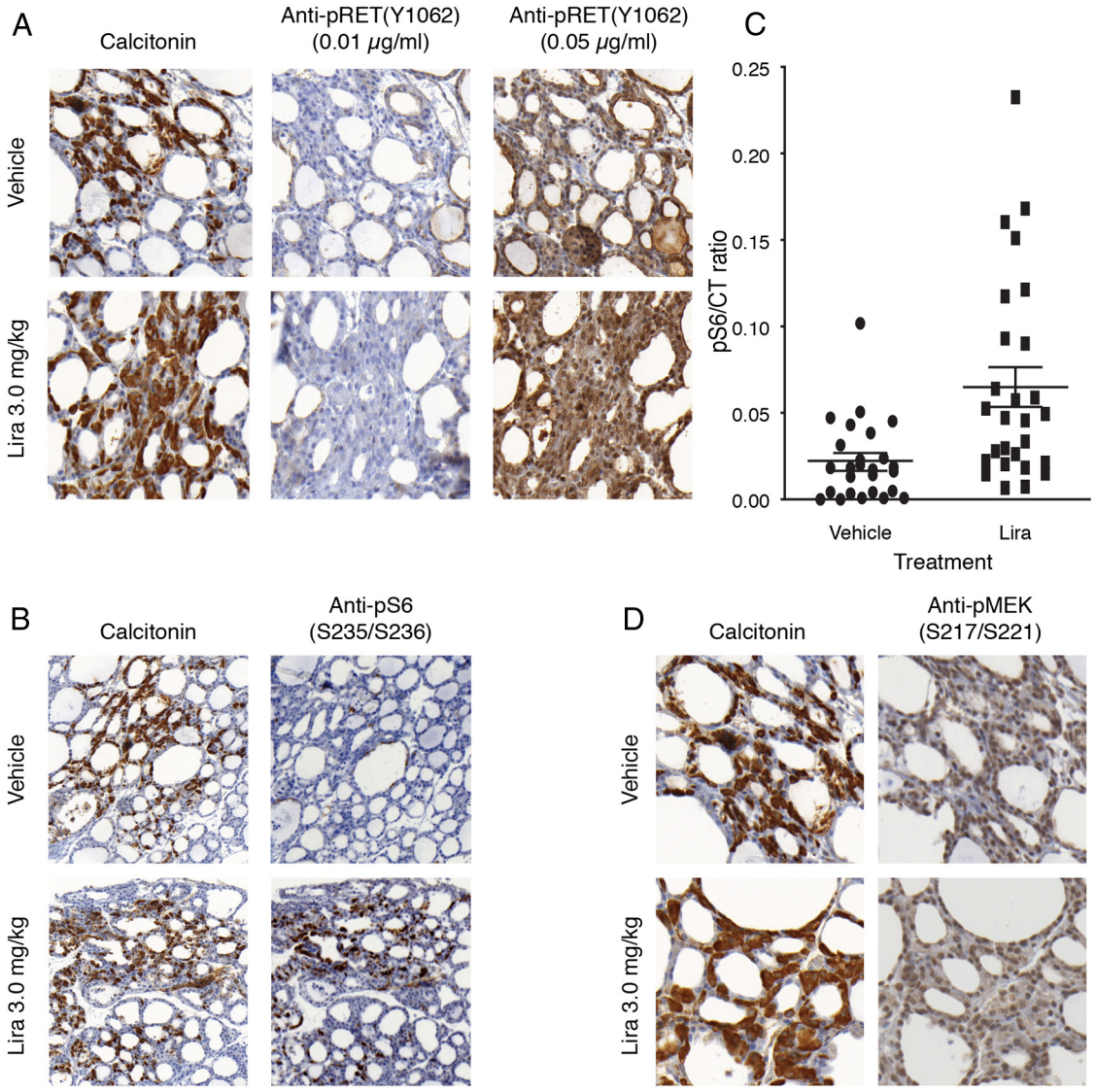

FIG. 5. IHC for phosphoproteins after 13 wk treatment with liraglutide (Lira, 3 mg/kg · d) in CD-1 wild-type mice. A, No up-regulation of pRET in calcitonin-positive cells in thyroids from liraglutide- *vs.* vehicle-treated mice. IHC is shown for pRET (Y1062) at 0.01 or 0.05 μg/ml in representative sections of thyroid tissue with C-cell hyperplasia from a liraglutide-treated mouse and a region with many C cells from a vehicle-treated mouse. B, Up-regulation of pS6 in calcitonin-positive cells in thyroids from liraglutide- *vs.* vehicle-treated mice. Representative IHC is shown for pS6 (S235/S236) and calcitonin performed on adjacent sections of thyroid tissue blocks of liraglutide- or vehicle-treated mice. C, Increased number of calcitonin- and pS6-positive cells in CD-1 mice treated with liraglutide (3 mg/kg · d) for 13 wk. *Bars* represent the ratio of pS6/calcitonin-positive cells. D, No up-regulation of pMEK in calcitonin-positive cells in thyroids from liraglutide- *vs.* vehicle-treated mice. Representative IHC is shown for pMEK (S217/S221) and calcitonin performed on adjacent sections of thyroid tissue blocks of liraglutide- or vehicle-treated mice.

data indicated an increased GLP-1R density in areas with C cells in mice dosed with liraglutide compared with vehicle controls. Although statistically significant, this difference was of limited magnitude (~30%) and did not show dose response, and the biological significance of the increase is not known.

TABLE 3. Incidence of IHC staining for RET, S6, and MEK phosphoproteins in C cells in CD-1 wild-type mice treated with liraglutide or vehicle for 13 wk

Treatment	Positive IHC/total examined		
	pRET	pMEK	pS6
Liraglutide vehicle	0/12	0/12	0/11
Liraglutide, 3.0 mg/kg · d	0/12	0/12	10/11

In the frozen thyroids with hyperplasia, ISLB analysis was performed on areas with normal C-cell density and compared with adjacent areas with C-cell hyperplasia in the same tissue sections. The analysis did not show any significant difference in C-cell GLP-1R density. However, the morphology of frozen sections was suboptimal for identifying these subtle changes, and because only 10 tissue samples with C-cell hyperplasia were suitable for the binding studies, we are reluctant to draw definitive con-

clusions based on this analysis. After agonist stimulation of GPCR, such as GLP-1R, both down-regulation and up-regulation has been described (26, 27). Although a recent study indicates potential higher C-cell GLP-1R density in rodents with hyperplastic *vs.* normal C cells (9), the reported magnitude of differences was limited, and a direct comparison in the same strain of animals was not made.

The objective of the thyroid RET IHC analysis was to determine whether GLP-1R agonist-induced C-cell hyperplasia in mice was associated with RET signaling. Expression of mutant RET in C cells of transgenic mice results in C-cell hyperplasia and neoplasms, indicating that RET activation can have transforming effects in rodents (28, 29). Ligand binding of GPCR can result in transactivation of receptor tyrosine kinases (30). Upon RET activation, phosphorylation can occur at different sites in the RET protein. Tyrosine phosphorylation at Y1062 is particularly critical for engaging key downstream signaling pathways, including MAPK, and for the growth-promoting effects of the receptor. Hence, in the present study, IHC was used to detect pRET (Y1062). There was no evidence of pRET staining in C cells, including C cells in areas of hyperplasia, indicating that liraglutide binding to the GLP-1R on C cells leading to C-cell hyperplasia in wild-type mice did not involve activation of RET. Although this analysis was confined to high-dose liraglutide animals only, the result is considered representative for GLP-1R agonist-induced C-cell findings in mice given the consistency of the GLP-1R agonist effects on C cells observed in this and in other studies (7).

pS6 results from upstream activation of mTOR, which controls cell growth in eukaryotes in response to nutrient availability and plays a role in regulating proliferation by growth factors, energy status, and stress conditions (31). Consistent with this, and the observed C-cell activation and hyperplasia, the C cells from liraglutide-treated mice had increased staining for pS6. Because mTOR integrates several different signaling pathways (16), this finding does not point to the precise upstream pathway responsible for increased C-cell proliferation. In pancreatic β-cells, GLP-1 activates mTOR by stimulating adenylyl cyclase to produce cAMP. GLP-1-induced mTOR, in turn, induces accumulation of the transcription factor hypoxia-inducible factor, which may promote islet cell viability through protection against oxidative stress (32). In contrast to the findings with pS6 IHC, we saw no increase in pMEK staining in the C-cell hyperplastic regions of liraglutide-treated mice. pMEK is a marker of the MAPK pathway, and the absence of pMEK activation is consistent with effects mediated via GLP-1R-cAMP-protein kinase A signaling, as opposed to activation of the MAPK pathway.

Long-term GLP-1R activation is associated with increased levels of calcitonin and tumor formation in rats and mice (7). We explored possible mechanisms behind these rodent findings and found a clear GLP-1R dependency of the C-cell stimulatory effects, that is, increased calcitonin and C-cell hyperplasia. In contrast, we found no evidence for activation of the *RET* protooncogene often involved in human MTC initiation. Our observations imply that the GLP-1R agonist-induced C-cell effects seen in rodents are associated with mTOR activation but that this is not linked to the RET pathway.

Acknowledgments

We accept direct responsibility for this paper and are grateful for the contributions made by Mellissa Chapman and Alan Broadmeadow (Huntingdon Life Sciences) for assistance with designing and conducting the animal experiments. Jonas Kildegaard is acknowledged for his expert assistance in setting up the morphometric analysis of the ISLB sections.

Address all correspondence and requests for reprints to: James A. Fagin, M.D., Memorial Sloan-Kettering Cancer Center, 1275 York Avenue, New York, New York 10065. E-mail: faginj@mskcc.org; or Lars W. Madsen, D.V.M., Ph.D., Novo Nordisk A/S, Novo Allé, DK-2880, Bagsvaerd, Denmark. E-mail: lwm@novonordisk.com.

This work was also supported by National Institutes of Health grant CA72597 (to J.A.F.).

L.W.M., J.A.K., and J.A.F. were involved in the study design and generation, analysis, and review of data and wrote the paper; C.G., A.P., I.S., S.A., L.A, K.M., A.B., and S.V. were involved in the generation of data; A.S.d.B., N.C.B.N., L.B.K., and A.M.M. were involved in discussion of the experimental set-up and data. All authors reviewed the paper and approved the final version.

Disclosure Summary: L.W.M. is employed by, has equity shares in, and has been a sponsor's representative for Novo Nordisk. J.A.K., A.P., K.M., A.B., and S.V. have nothing to disclose. C.G. is employed by, has equity shares in, and is a coauthor on one patent with Novo Nordisk. I.S., L.A., S.A., A.S.d.B., N.C.B.N., and A.M.M. are employed by and have equity shares in Novo Nordisk. L.B.K. is the inventor of liraglutide in the patents held by Novo Nordisk but has no personal rights; she is employed by and has equity shares in Novo Nordisk. J.A.F. received grant support in 2010 from and has previously consulted for Novo Nordisk.

References

1. **Garber AJ** 2011 Long-acting glucagon-like peptide 1 receptor agonists: a review of their efficacy and tolerability. Diabetes Care 34(Suppl 2):S279–S284
2. **Buse JB, Rosenstock J, Sesti G, Schmidt WE, Montanya E, Brett JH, Zychma M, Blonde L; LEAD-6 Study Group** 2009 Liraglutide once

a day versus exenatide twice a day for type 2 diabetes: a 26-week, randomised, parallel-group, multinational, open-label trial (LEAD-6). Lancet 374:39–47

3. **Buse JB, Nauck MA, Forst T, Sheu WHH, Hoogwerf BJ, Shenouda SK, Heilmann CR, Boardman MK, Fineman M, Porter L, Schernthaner G** 2011 Efficacy and safety of exenatide once weekly versus liraglutide in subjects with type 2 diabetes (DURATION-6): a randomised, open-label study. Diabetologia 54(Suppl 1):S38 (Abstract 75)
4. **European Medicines Agency (EMA)** 2006: Assessment report for Byetta http://www.ema.europa.eu/docs/en_GB/document_library/EPAR_-_Scientific_Discussion/human/000698/WC500051842.pdf (accessed Sept 27, 2011)
5. **European Medicines Agency (EMA)** 2009: Assessment report for Victoza http://www.ema.europa.eu/docs/en_GB/document_library/EPAR_-_Public_assessment_report/human/001026/WC500050016.pdf (accessed Sept 27, 2011)
6. **European Medicines Agency (EMA)** 2011: Assessment report for Bydureon http://www.ema.europa.eu/docs/en_GB/document_library/EPAR_-_Public_assessment_report/human/002020/WC500108239.pdf (accessed Sept 27, 2011)
7. **Bjerre Knudsen L, Madsen LW, Andersen S, Almholt K, de Boer AS, Drucker DJ, Gotfredsen C, Egerod FL, Hegelund AC, Jacobsen H, Jacobsen SD, Moses AC, Mølck AM, Nielsen HS, Nowak J, Solberg H, Thi TD, Zdravkovic M** 2010 Glucagon-like peptide-1 receptor agonists activate rodent thyroid C-cells causing calcitonin release and C-cell proliferation. Endocrinology 151:1473–1486
8. **Hegedüs L, Moses AC, Zdravkovic M, Le Thi T, Daniels GH** 2011 GLP-1 and calcition concentration in humans: Lack of evidence of calcitonin release from sequential screening in over 5000 subjects with type 2 diabetes or nondiabetic obese subjects treated with the human GLP-1 analog, liraglutide. J Clin Endocrinol Metab 96:853–860
9. **Waser B, Beetschen K, Pellegata NS, Reubi JC** 2011 Incretin receptors in non-neoplastic and neoplastic thyroid C cells in rodents and humans: relevance for incretin-based diabetes therapy. Neuroendocrinology 94:291–301
10. **Parks M, Rosebraugh C** 2010 Weighing risks and benefits of liraglutide: The FDA's review of a new antidiabetic therapy. N Engl J Med 362:774–777
11. **Aschebrook-Kilfoy B, Ward MH, Sabra MM, Devesa SS** 2011 Thyriod cancer incidence patterns in the United States by histologic type, 1992–2006. Thyroid 21:125–134
12. **Wells Jr SA, Santoro M** 2009 Targeting the RET pathway in thyroid cancer. Clin Cancer Res 15:7119–7123
13. **Asai N, Murakami H, Iwashita T, Takahashi M** 1996 A mutation at tyrosine 1062 in MEN2A-Ret and MEN2B-Ret impairs their transforming activity and association with shc adaptor proteins. J Biol Chem 271:17644–17649
14. **Salvatore D, Melillo RM, Monaco C, Visconti R, Fenzi G, Vecchio G, Fusco A, Santoro M** 2001 Increased in vivo phosphorylation of ret tyrosine 1062 is a potential pathogenetic mechanism of multiple endocrine neoplasia type 2B. Cancer Res 61:1426–1431
15. **Mayo KE, Miller LJ, Bataille D, Dalle S, Göke B, Thorens B, Drucker DJ** 2003 International Union of Pharmacology. XXXV. The glucagon receptor family. Pharmacol Rev 55:167–194
16. **Kwon G, Marshall CA, Pappan KL, Remedi MS, McDaniel ML** 2004 Signalling elements involved in the metabolic regulation of mTOR by nutrients, incretins, and growth factors in islets. Diabetes 53(Suppl 3):S225–S232
17. **DeLellis RA** 1994 Changes in structure and function of thyroid C-cell. In: Mohr U, Dungworth DL, Capen CC, eds. Pathobiology of the aging rat. 2nd ed. Washington, DC: International Life Sciences Institute; 285–299
18. **Botts S, Jokinen MP, Isaacs KR, Meuten DJ, Tanaka N** 1991 Proliferative lesions of the thyroid and parathyroid glands, E-3. In: Guides for toxicologic pathology. Washington, DC: STP/ARP/AFIP; 1–12
19. **Boorman GA, DeLellis RA, Elwell MR** 1996 C-cell hyperplasia, C-cell adenoma, and C-cell carcinoma, thyroid in rats. In: Jones TC, Capen CC, Mohr U, eds. Endocrine system ILSI monographs on laboratory animals. 2nd ed. Heidelberg: Springer-Verlag; 262–273
20. **Ishizaka Y, Ushijima T, Sugimura T, Nagao M** 1990 cDNA cloning and characterization of ret activated in a human papillary thyroid carcinoma cell line. Biochem Biophys Res Commun 168:402–408
21. **Powell Jr DJ, Russell J, Nibu K, Li G, Rhee E, Liao M, Goldstein M, Keane WM, Santoro M, Fusco A, Rothstein JL** 1998 The RET/PTC3 oncogene: metastatic solid-type papillary carcinomas in murine thyroids. Cancer Res 58:5523–5528
22. **Akeno-Stuart N, Croyle M, Knauf JA, Malaguarnera R, Vitagliano D, Santoro M, Stephan C, Grosios K, Wartmann M, Cozens R, Caravatti G, Fabbro D, Lane HA, Fagin JA** 2007 The RET kinase inhibitor NVP-AST487 blocks growth and calcitonin gene expression through distinct mechanisms in medullary thyroid cancer cells. Cancer Res 67:6956–6964
23. **Körner M, Stöckli M, Waser B, Reubi JC** 2007 GLP-1 receptor expression in human tumors and human normal tissues, potential for in vivo targeting. J Nucl Med 48:736–743
24. **Hebel R, Stromberg MW** 1986 Anatomy and embryology of the laboratory rat. Wörthsee, Germany: BioMed Verlag; 91
25. **Lindfors PH, Lindahl M, Rossi J, Saarma M, Airaksinen MS** 2006 Ablation of persephin receptor glial cell-line derived neurotrophic factor family receptor α4 impairs thyroid calcitonin production in young mice. Endocrinology 147:2237–2244
26. **Tanowitza M, von Zastrow M** 2010 Agonist-induced desensitization and endocytosis of G-protein-coupled receptors. In: Bradshaw RA, Dennis EA. Handbook of cell signalling. 2nd ed. Amsterdam: Elsevier Press; 177–183
27. **Ramírez JL, Watt HL, Rocheville M, Kumar U** 2005 Agonist-induced up regulation of human somatostatin receptor type 1 is regulated by β-arrestin-1 and requires an essential serine residue in the receptor C-tail. Biochim Biophys Acta 1669:182–192
28. **Acton DS, Velthuyzen D, Lips CJ, Höppener JW** 2000 Multiple endocrine neoplasia type 2B mutation in human RET oncogene induces medullary thyroid carcinoma in transgenic mice. Oncogene 19:3121–3125
29. **Michiels FM, Chappuis S, Caillou B, Pasini A, Talbot M, Monier R, Lenoir GM, Feunteun J, Billaud M** 1997 Development of medullary thyroid carcinoma in transgenic mice expressing the RET protooncogene altered by a multiple endocrine neoplasia type 2A mutation. Proc Natl Acad Sci USA 94:3330–3335
30. **Daub H, Weiss FU, Wallasch C, Ullrich A** 1996 Role of transactivation of the EGF receptor in signalling by G-protein-coupled receptors. Nature 379:557–560
31. **Sengupta S, Peterson TR, Sabatini DM** 2010 Regulation of the mTOR complex 1 pathway by nutrients, growth factors, and stress. Mol Cell 40:310–322
32. **Van de Velde S, Hogan MF, Montminy M** 2011 mTOR links incretin signaling to HIF induction in pancreatic β-cells. Proc Natl Acad Sci USA 108:16876–16882